

# A multi-mode delay differential equation model for lasers with optical feedback

Mindaugas Radziunas

Weierstrass Institute, Mohrenstrasse 39, 10117 Berlin, Germany. Email: Mindaugas.Radziunas@wias-berlin.de

In this work, we introduce a new multi-mode (MM) delay differential equation (DDE) model suited for simulations of the Fabry-Perot type diode laser with an optical feedback from the external cavity (EC), see Fig. 1(a).

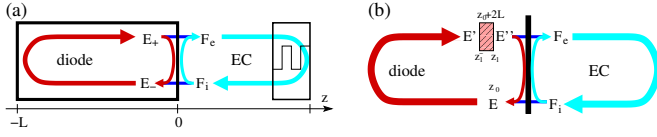


Fig. 1. Schematic representations of the diode laser with an external cavity. (a): linear configuration, as considered in the TW model. (b): ring diode laser configuration (left) with a localized filtering element (hatched box) and the filtered optical feedback from the external cavity (right), as considered in the new MMDDE model.

To demonstrate advantages of this new model, we consider and compare three models describing nonlinear dynamics of complex slowly varying amplitudes of optical fields  $E$  and carrier densities  $n$  in the FP laser with a simple EC. Our basic approach is given by the traveling wave (TW) model, which is a 1(space)+1(time) dimensional system of partial differential equations describing the longitudinal and temporal evolution of counter-propagating optical fields,  $E_+$  and  $E_-$ , and dynamics of spatially averaged carrier density [1]. Another approach is a well-known delay differential equation (DDE) model of Lang-Kobayashi (LK) type, which was originally used for investigation of dynamics in single-mode lasers with *long* ECs and *weak* optical feedback [2]. The last MMDDE model proposed in this work is derived from the TW model under assumptions of ring configuration of the diode laser and unidirectional propagation of the optical field within this ring, see Refs. [3], [4] and Fig. 1(b). In contrast to the LK type models, this MMDDE model properly accounts for multiple longitudinal modes of the diode laser and, therefore, admits considering *moderate* and *strong* optical feedback regimes. Such kind of feedback is typical for a large class of external cavity diode lasers, where the optical length of the EC is comparable to the diode length [5], whereas the field reflectivity at the rear facet of the diode is reduced, such that the solitary lasing can be achieved only at very high bias currents. On the other hand, comparing to the TW model, our new MMDDE model is relatively simple and admits fast numerical integration, numerical bifurcation analysis, and more detailed analytic investigations.

*External cavity.* In all three cases, we assume that the action of the EC, i.e., the relation between the optical field  $F_i(t)$  re-injected into the diode and the field  $F_e(t)$  emitted from the diode is given by the linear operator  $\mathcal{F}$ . For the simple EC determined by an external mirror,  $\mathcal{F}$  is, basically, a simple

time-delay operator:

$$F_i(t) = [\mathcal{F}F_e](t) = K e^{i\phi} F_e(t-\tau), \quad (1)$$

where  $\tau$  is the field round-trip time in the EC, whereas  $K$  and  $\phi$  are the transmission factor and the phase shift of the complex field amplitude during this round-trip. More sophisticated ECs can contain several reflectors or different frequency filtering elements, such as passive resonators or Bragg gratings. The action of various objects of the EC can be approximated by linear continuous time filters described by ODEs. For example, the delay operator (1) can be interpreted as a broad Lorentzian filter,

$$\begin{aligned} F_i(t) &= [\mathcal{F}F_e](t) = \tilde{\gamma} K e^{i\phi} \int_{-\infty}^{t-\tau} e^{-\tilde{\gamma}(t-\tau-\nu)} F_e(\nu) d\nu \\ \Rightarrow \frac{1}{\tilde{\gamma}} \frac{d}{dt} F_i(t) &= K e^{i\phi} F_e(t-\tau) - F_i(t), \end{aligned} \quad (2)$$

in the limit case of  $\tilde{\gamma} \rightarrow +\infty$ . For the sake of simplicity, we consider only the simplest case of the EC determined by Eq. (1) or Eq. (2) in this work.

*Traveling wave model.* After a suitable normalization [6], the spatially-distributed TW model within the laser diode can be written as

$$\begin{aligned} (\partial_t \pm \partial_z) E_{\pm} &= \left( (1 + i\alpha_H) n - \frac{\xi_0}{L} - \mathcal{P} \right) E_{\pm}, \\ \mathcal{P} E_{\pm} &= \frac{\bar{q}}{2} (E_{\pm} - P_{\pm}), \quad \frac{d}{dt} P_{\pm} = \bar{\gamma} E_{\pm} + (i\bar{\omega} - \bar{\gamma}) P_{\pm}, \\ \epsilon^{-1} \frac{d}{dt} n &= J - n - \Re \langle (E, [2n + 1 - 2\mathcal{P}] E) \rangle, \end{aligned} \quad (3)$$

where  $E = (E_+, E_-)^T$ ,  $(\cdot, \cdot)$  and  $\langle \cdot \rangle$  are scalar product of vector functions and spatial average, respectively. The complex factor  $\xi_0$  is determined by the relation  $e^{2\xi_0} = -r_f^* r_r e^{-2\chi(0)}$ , where  $r_f$  and  $r_r$  are complex field amplitude reflection coefficients at the front ( $z = -L$ ) and rear ( $z = 0$ ) diode facets, whereas  $\chi(\omega) = \frac{\bar{q}L}{2} \frac{i(\omega - \bar{\omega})}{\bar{\gamma} + i(\omega - \bar{\omega})}$ . To close the model equations, we define the following field reflection-transmission-reinjection conditions at the diode facets:

$$\begin{aligned} E_+(-L, t) &= -r_f^* E_-(-L, t), \\ \begin{pmatrix} F_e(t) \\ E_-(0, t) \end{pmatrix} &= \begin{pmatrix} t_r & -r_r^* \\ r_r & t_r \end{pmatrix} \begin{pmatrix} E_+(0, t) \\ F_i(t) \end{pmatrix}, \end{aligned} \quad (4)$$

where  $t_r = \sqrt{1 - |r_r|^2}$  is the field transmission through the rear facet, whereas  $F_e$  and  $F_i$  are related by Eq. (1).

*Lang-Kobayashi type model.* The normalized LK type model can be written as

$$\begin{aligned} \frac{d}{dt} E &= (1 + i\alpha_H) n E + C F_i, \quad F_i(t) = [\mathcal{F}E](t), \\ \epsilon^{-1} \frac{d}{dt} n &= J - n - (2n + 1) |E|^2, \end{aligned} \quad (5)$$

where the operator  $\mathcal{F}$  and parameters  $J$ ,  $\epsilon$  and  $\alpha_H$  are the same as in the TW model discussed above. The coefficient

$C = \frac{t_r^2}{2r_r L}$  relates the feedback rate (which in non-scaled LK model would have the dimension  $s^{-1}$ ) with the dimensionless field transmission factor  $Ke^{i\phi}$  from (1) [6].

*Multi-mode DDE model.* Following Ref. [3], we neglect back propagating field  $E_-$  in the TW model, assume the ring configuration of the diode laser, and allow the spatial distribution of carriers. We assume that all distributed field amplitude losses, frequency detuning, and field dispersion within the diode are concentrated within a single point source [hatched box in Fig. 1(b)], whereas the relation of the incident and transmitted fields  $E'(t)$  and  $E''(t)$  [see notations in Fig. 1(b)] are defined by

$$\frac{d}{dt}E''(t) = (\gamma' - i\bar{\omega})(\mu E'(t - \Delta) - E''(t)), \quad \text{where}$$

$$\gamma' = \frac{\tilde{\gamma}}{\sqrt{2g}L}, \quad \mu = \frac{e^{-(1+i\alpha_H)L}}{r_r}, \quad \Delta = \frac{gL - \sqrt{2g}L}{\tilde{\gamma}} = \tau_d - 2L.$$

After introducing forward along the characteristic line performed sliding average  $\tilde{n}(t) = \frac{1}{2L} \int_{z_0}^{z_1} n(\nu, t + \nu - z_0) d\nu$ , resolving the unidirectional TW equation, eliminating  $E'$ ,  $E''$ ,  $F_e$ , and introducing new function  $F = \frac{1}{t_r} F_i$ , we obtain the following MMDDE model for lasers with an external feedback:

$$\begin{aligned} \frac{d}{dt}E &= -[\gamma' - i\bar{\omega}]E(t) + t_r^2[\gamma' - i\bar{\omega} - \tilde{\gamma}]F(t) \\ &\quad + t_r^2 \frac{\tilde{\gamma}Ke^{i\phi}}{r_r} [E(t - \tau) - F(t - \tau)] \\ &\quad + (\gamma' - i\bar{\omega})e^{(1+i\alpha_H)\tilde{n}(t - \tau_d)2L} E(t - \tau_d), \quad (6) \\ \frac{d}{dt}F &= -\tilde{\gamma}F(t) + \frac{\tilde{\gamma}Ke^{i\phi}}{r_r} [E(t - \tau) - F(t - \tau)], \\ \epsilon^{-1} \frac{d}{dt}\tilde{n} &= J - \tilde{n} - \frac{1}{2L} [e^{[2\tilde{n}+1]2L} - 1] |E|^2. \end{aligned}$$

*Comparison of models.* Cavity modes (CMs) play a significant role determining dynamics of the lasers with an external feedback. The CMs, which are the steady states of the corresponding system, can be defined by the threshold carrier density  $\bar{n}$  and the relative optical frequency  $\omega$ . The choice of the scaling factor  $C$  in the LK model [6] and the parameters  $\gamma'$ ,  $\mu$ ,  $\Delta$  in the MMDDE model allow to get a best fitting of the CMs in the reduced DDE models to the CMs of the TW model.

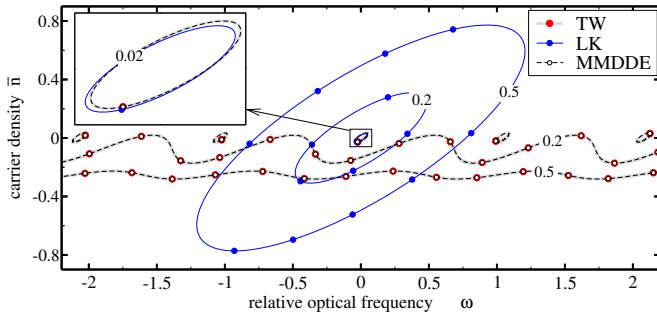


Fig. 2. Curves of CMs in the TW (thick grey), LK (thin solid) and MMDDE (thin dashed) models for arbitrary  $\phi$  and  $K = 0.02$ ,  $K = 0.2$ , and  $K = 0.5$ , whereas  $L = 3$ ,  $\tau = 13.5$ ,  $\alpha_H = 1.2$ ,  $r_f = \sqrt{0.3}$ ,  $r_r = e^{-2.84}/r_f \approx 0.1$ ,  $\bar{\omega} = 0$ ,  $g = 6$ ,  $\tilde{\gamma} = 120$ ,  $\tilde{\gamma} = 500$ . Bullets on the corresponding curves show location of the cavity modes for fixed  $\phi = 0$ . An insert shows enlarged curves for  $K = 0.02$  in the vicinity of origin,  $(\omega, \bar{n}) = (0, 0)$ .

Different curves in Fig. 2 represent all possible locations of the CMs for fixed feedback amplitude factor  $K$  and arbitrary feedback phase  $\phi$ . It can be clearly seen, that for small  $K$ ,

the CMs of the LK model provide a good approximation of the CMs of the TW model in the vicinity of the origin  $(\omega, \bar{n}) = (0, 0)$ , see thin blue and thick grey solid curves within the insert of Fig. 2. We note, however, that for small  $K$  and fixed  $\phi$ , the LK modes has a unique CM (blue diamond in Fig. 2), whereas the TW model possesses multiple CMs with similar separation ( $\sim \pi/L$ ) of mode frequencies  $\omega$  and similar thresholds  $\bar{n}$  (red bullets in Fig. 2). For moderate and large  $K$ , the agreement between LK and TW equations is drastically degraded: whereas CMs of the LK model are located on the increasing ellipses centered around the origin  $(0, 0)$ , the CMs of the TW model are on a single, only slightly undulated nearly horizontal non-connected curve. In contrast, the CMs of our new MMDDE model are in nearly perfect agreement with the CMs of the TW model for all values of  $K$ : see indistinguishable thin dashed and thick grey curves in Fig. 2.

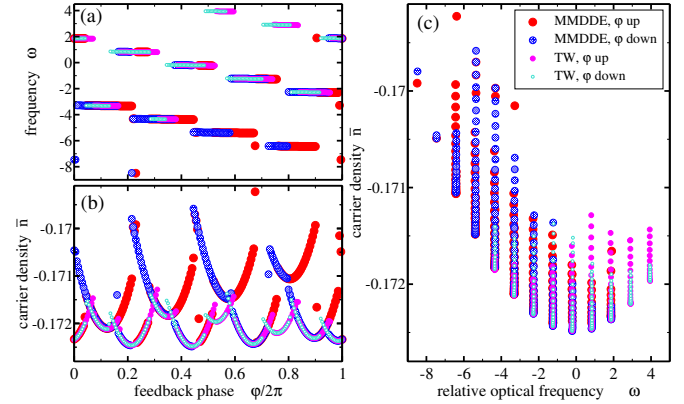


Fig. 3. Changes of states during numerical integration of the TW and MMDDE with increased and decreased  $\phi$ . (a) and (b): main frequency and mean carrier density as functions of  $\phi$ . (c): same calculations in frequency-carrier density plane.  $K = 0.2$ ,  $J = 2$ ,  $\epsilon = 4 \cdot 10^{-3}$ , whereas other parameters as in Fig. 2.

Another comparison of the MMDDE and TW models is presented in Fig. 3. Here, we have performed estimation of the states for different values of the feedback phase factor  $\phi$  using direct numerical integration of two different models. Panels (a) and (b) of this figure show the observed multiple transitions between different CMs. All observed states are also indicated by different bullets in frequency-carrier density plane (panel (c) of the same figure). It is noteworthy that all these states represent only those CMs which are located close to the multiple-minima of the thick solid and thin dashed curves corresponding to the case  $K = 0.2$  in Fig. 2. The frequency separation of these states is, approximately,  $\pi/L$ , what correspond to the separation of the FP laser resonances.

## REFERENCES

- [1] U. Bandelow et al., *IEEE J. of Quantum Electron.* **37**, p. 183, 2001
- [2] R. Lang and K. Kobayashi, *IEEE J. of Quantum Electron.* **16**, p. 347, 1980
- [3] A.G. Vladimirov and D. Turaev, *Phys. Rev. A* **72**, p. 033808, 2005
- [4] R.M. Arkhipov et al., *Appl. Phys. B* **118**, p. 539, 2015
- [5] M. Radziunas et al. *IEEE J. of Quantum Electron.* **51**, p. 2000408, 2015
- [6] M. Radziunas et al., *SPIE Proceedings Series* **6184**, p. 61840X, 2006